

# Dynamic behavior of a hydraulic crane operating a freely suspended payload

Bozhidar GRIGOROV, Rosen MITREV

**Cite this as:** Bozhidar GRIGOROV, Rosen MITREV, 2017. Dynamic behavior of a hydraulic crane operating a freely suspended payload. *Journal of Zhejiang University-SCIENCE A (Applied Physics & Engineering)*, 18(4):268-281. <http://dx.doi.org/10.1631/jzus.A1600292>

# Introduction

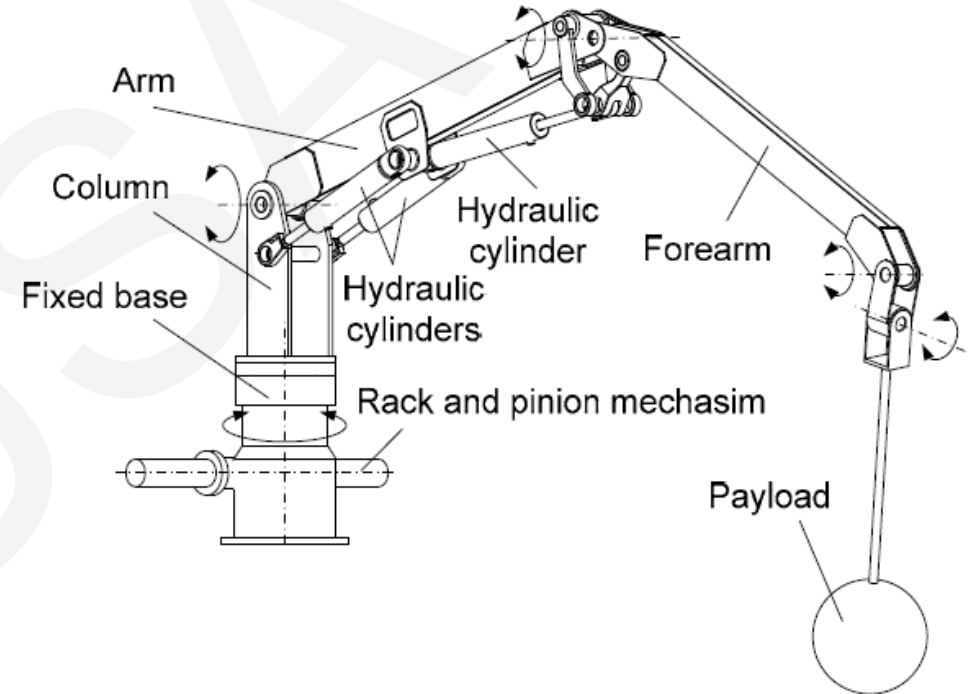
Hydraulically driven cranes are materials handling equipment used in many areas where compact devices are needed to manipulate heavy loads, typically in automobile, railroad, or sea transport. Dynamical modeling of hydraulic cranes is essential for their designers because of the need to reduce manufacturing costs and to gain better insight over the behavior of the designed mechanical system.

## Aim of the present study

The general aim of the present study is to investigate the dynamic behavior of a hydraulically driven crane with an articulated boom and a freely suspended payload at its end. The investigation is directed towards the worst case of hydraulic flow control, i.e., sudden opening and closure of hydraulic valves. To simplify the problem, two motions of the crane boom, namely luffing and slewing, are considered separately. This generally reduces the case to the dynamics of luffing jib cranes and slewing cranes.

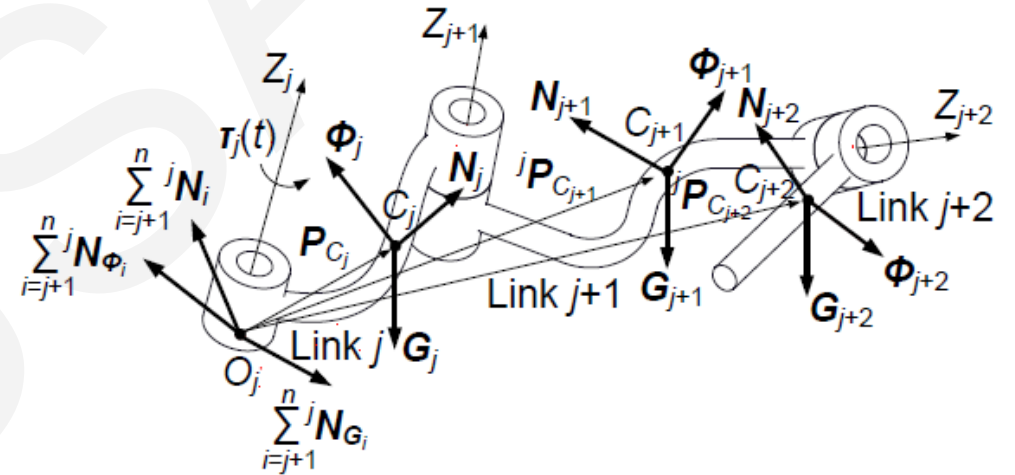
# General model of the mechanical system

Fig. 1 shows a discrete 3D model of a hydraulic rotating crane with an articulated boom and a freely suspended payload. The crane consists of a fixed base and three rotating links. The column rotates about the vertical axis and the boom is composed of an arm and a forearm, both rotating about horizontal axes to determine the reach of the crane and the payload lift respectively. To simulate the spatial sway of the payload, two additional rotational joints are added to the forearm, both having mutually perpendicular axes of rotation. The crane hydraulic drive system consists of a rack and pinion mechanism, intended for column rotation, and hydraulic cylinders, intended for arm and forearm rotation.



**Fig. 1 Discrete 3D model of the hydraulic crane**

To compose the set of differential equations of motion, a non-iterative method proposed in Grigorov (2013) is used. The method is based on a general Newton-Euler algorithm for solving the forward dynamics problem of an open kinematic chain with revolute joints. It is based on D'Alembert's principle, which implies that the dynamic balance of each link  $j$  (Fig. 2) is considered during the entire motion and with all the forces and moments acting on the link, including inertial, gravity, and the actuator torque.



**Fig. 2 Local frames and forces acting on the kinematic chain links**

# Slewing case

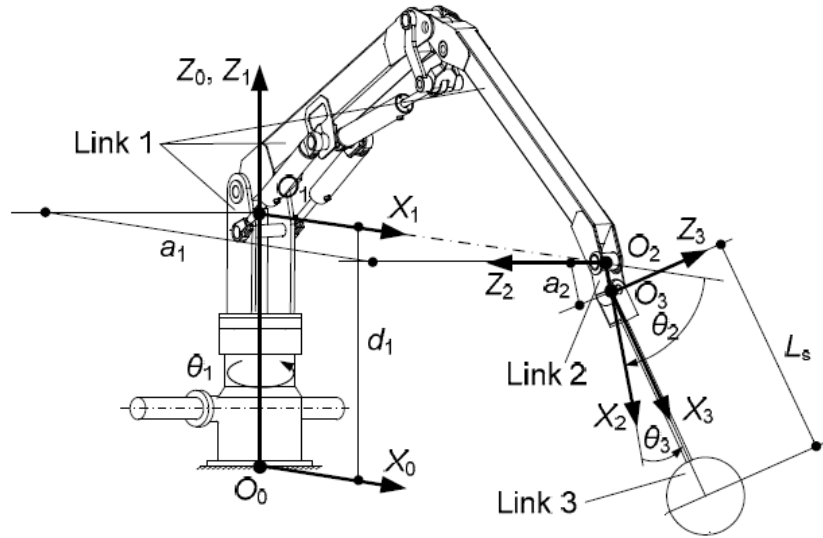


**Fig. 3 Denavit-Hartenberg (D-H) parameters and frame attachment for the slewing case**

**Table 1 Denavit-Hartenberg (D-H) parameters for the slewing case**

Link $j$	$\alpha_j$ (rad)	$a_j$ (m)	$d_j$ (m)	$\theta_j$ (rad)
1	0	0	Min: -1.22; Max: 1.18	$\theta_1$
2	$\pi/2$	Min: 2.037; Max: 3.352	0	$\theta_2$
3	$-\pi/2$	0.162	0	$\theta_3$

Max or min refers to the maximum or the minimum reach of the crane

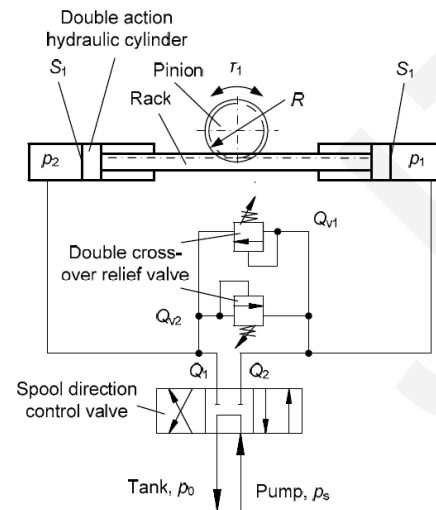


**Fig. 4 Slewing hydraulic rack and pinion mechanism**

# Luffing case

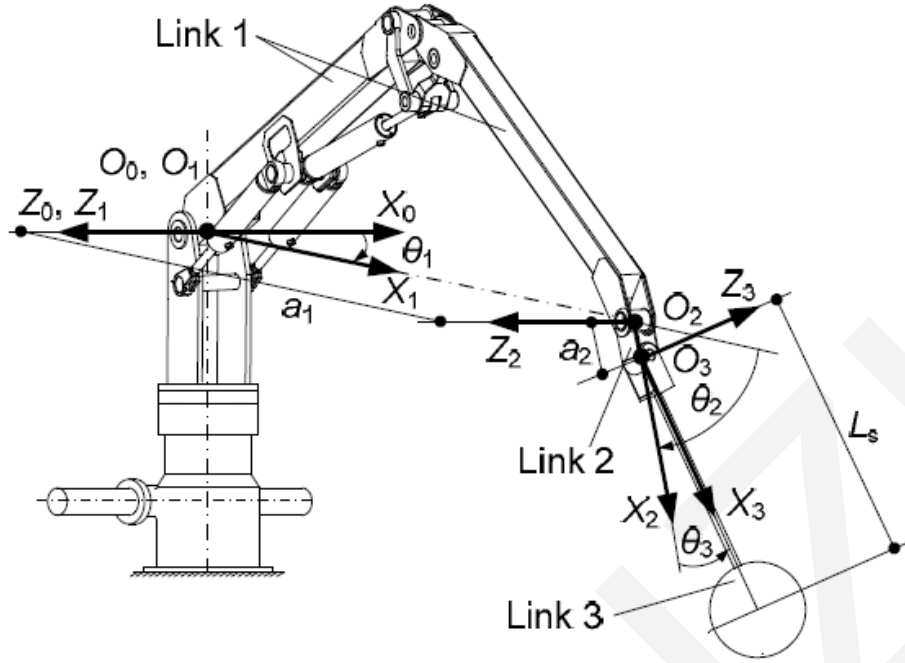


**Fig. 5 Denavit-Hartenberg (D-H) parameters and frame attachment for the luffing case**

**Table 2 Denavit-Hartenberg (D-H) parameters for the luffing case**

Link $j$	$\alpha_j$ (rad)	$a_j$ (m)	$d_j$ (m)	$\theta_j$ (rad)
1	0	0	0	$\theta_1$
2	0	3.352	0	$\theta_2$
3	$-\pi/2$	0.162	0	$\theta_3$

# Numerical examples

**Table 3 Numerical values for the mass and mass moments of inertia of the crane elements**

Link $j$	Mass, $m_j$ (kg)		Inertia tensor $I_j$ elements on the main diagonal (kg·m <sup>2</sup> )	
	Luffing	Slewing	Luffing	Slewing
1	$m_1=128.1$	$m_1=277.3$	$J_{xx}=1.4, J_{yy}=95, J_{zz}=94$	Minimum reach: $J_{xx}=65.9, J_{yy}=193.0, J_{zz}=131.0$ ; Maximum reach: $J_{xx}=41.8, J_{yy}=274.5, J_{zz}=236.2$
2	$m_2=5.9$	$m_2=5.9$	$J_{xx}=0.016, J_{yy}=0.032, J_{zz}=0.027$	$J_{xx}=0.016, J_{yy}=0.032, J_{zz}=0.027$
3	$m_3=150.3$	$m_3=150.3$	$J_{xx}=4.1, J_{yy}=9.2, J_{zz}=9.2$	$J_{xx}=4.1, J_{yy}=9.2, J_{zz}=9.2$

**Table 4 Numerical values for the hydraulic system parameters**

Parameter	Value	Parameter	Value
Relief valve preset pressure, $p_{set}$	9 MPa	Drain pressure, $p_0$	0
Supply pressure, $p_s$	8 MPa (slewing), 18 MPa (luffing)	Opening and closing time of the directional valve	0.05 s
Fluid bulk modulus, $\beta$	$1.32 \times 10^9$ Pa	Orifice discharge coefficient, $C_d$ or $C_{dv}$	0.62
Relief valve regulation range, $p_{reg}$	0.5 MPa	Hydraulic cylinder strokes	$l_1=0.5$ m, $l_2=0.38$ m
Valve pressure at maximum opening, $p_{max}$	9.5 MPa	Radius of the pinion, $R$	0.12 m
Fully open relief valve passage area, $A_{max}$	$1.2 \times 10^{-4}$ m <sup>2</sup>	Direction control valve area gradient, $w$	0.011 m
Constant oil volumes	$V_0^1 = 18.2 \times 10^{-6}$ m <sup>3</sup> , $V_0^2 = 42.9 \times 10^{-6}$ m <sup>3</sup>	The maximum direction control valve opening, $x_v^{max}(t)$	$0.5 \times 10^{-3}$ m
Piston areas	$S_1=1.96 \times 10^{-3}$ m <sup>2</sup> , $S_2=7.69 \times 10^{-3}$ m <sup>2</sup> , $S_3=3.04 \times 10^{-3}$ m <sup>2</sup>	Viscous friction coefficients	$b_1=1.2 \times 10^6$ N·s/m, $b_2=2.2 \times 10^6$ N·s/m
Fluid density, $\rho$	855 kg/m <sup>3</sup>		

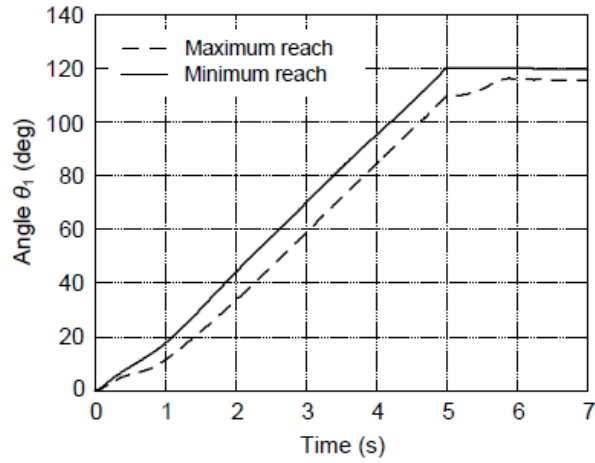


Fig. 7 Slewing angle  $\theta_1$

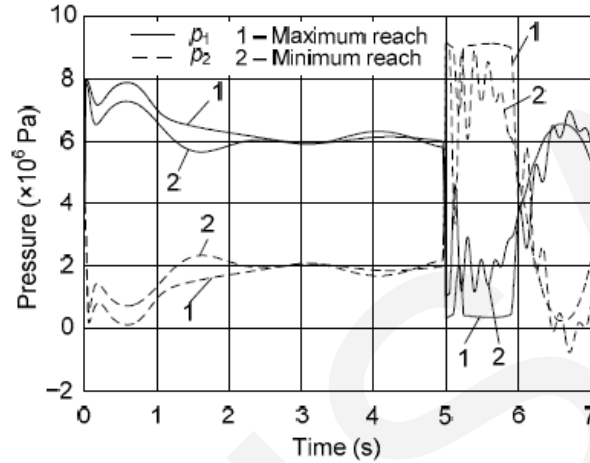


Fig. 9 Hydraulic cylinder pressure

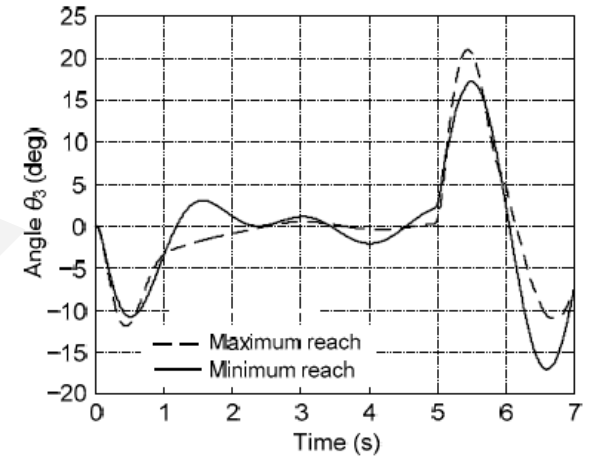


Fig. 11 Angle  $\theta_3$

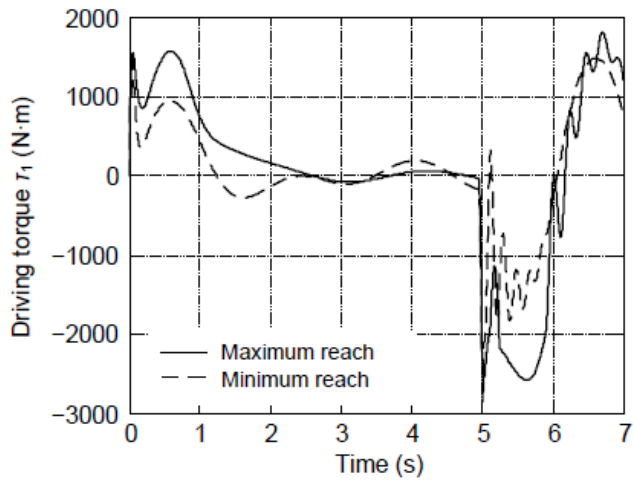


Fig. 8 Driving torque  $\tau_1$  exerted at the first link

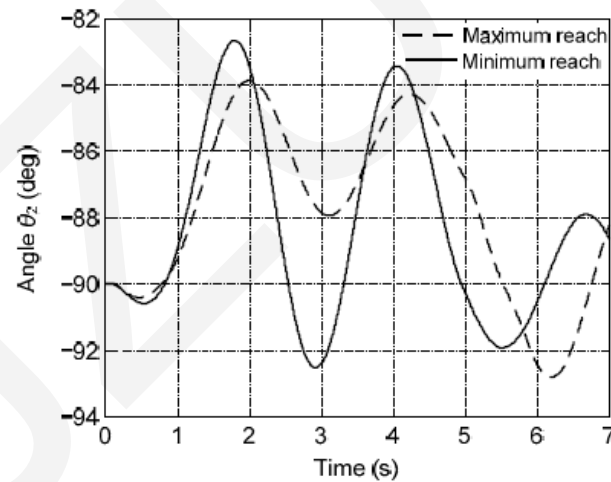


Fig. 10 Angle  $\theta_2$

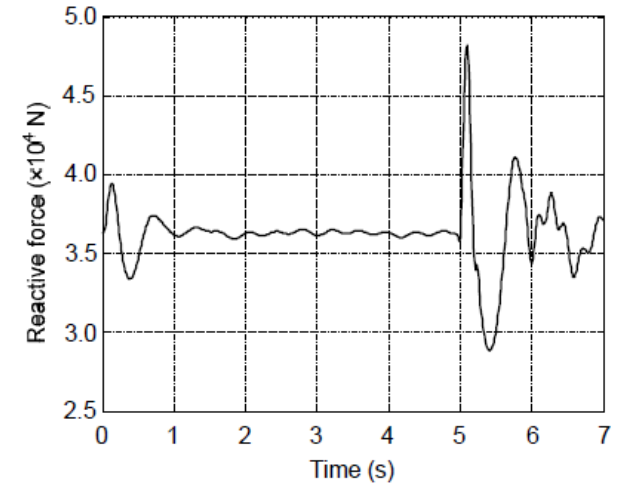
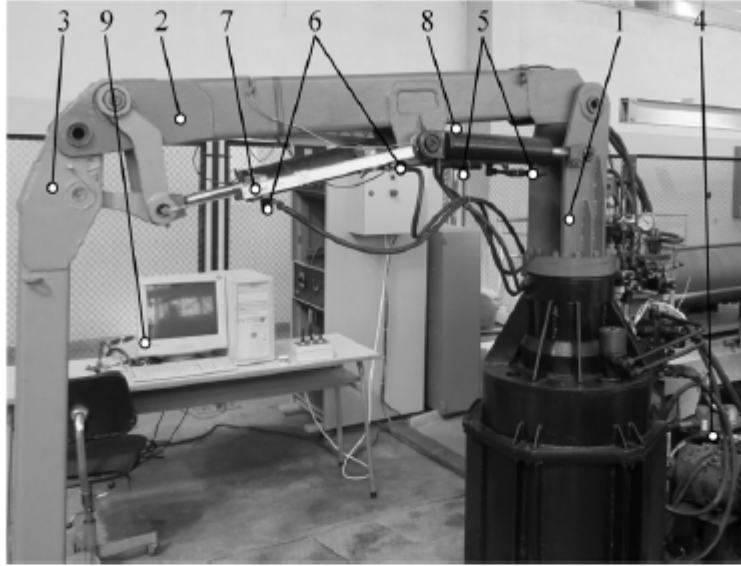
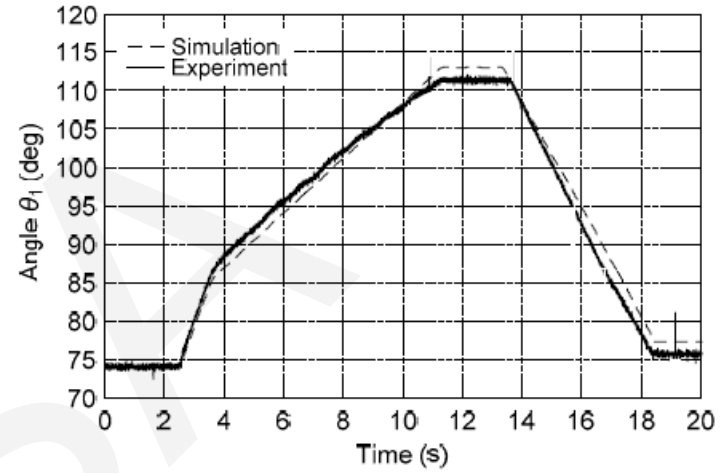


Fig. 12 Reactive force in the forearm hydraulic cylinder at the maximum reach



**Fig. 16** A view of the experimental setup and sensor placement

1: rotating column; 2: arm; 3: forearm; 4: hydraulic power unit; 5: sensors for measuring the pressures at the cap end and at the rod end of the arm driving cylinder; 6: sensors for measuring the pressures at the cap end and at the rod end of the forearm driving cylinder; 7: sensor for measuring the current displacement of the arm driving cylinder; 8: sensor for measuring the current displacement of the forearm driving cylinder; 9: computer measurement system



**Fig. 17** Time history of the boom rotation angle  $\theta_1$  for the luffing case

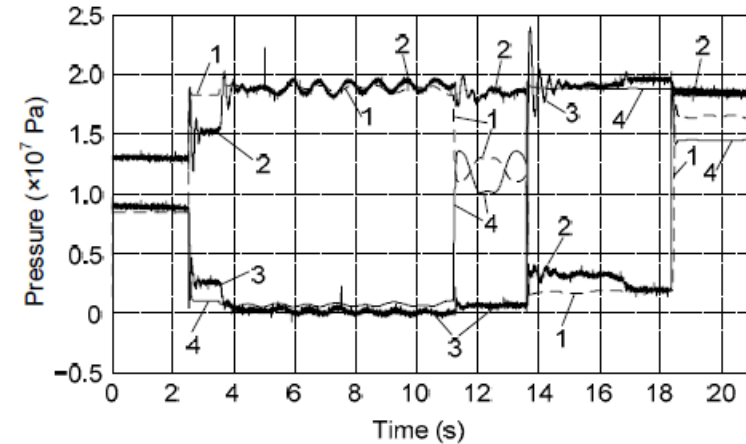


**Fig. 18** Pressures in the boom hydraulic cylinder for the luffing case

1: simulation data for  $p_1$ ; 2: experimental data for  $p_1$ ; 3: experimental data for  $p_2$ ; 4: simulation data for  $p_2$

# Conclusions

The design process for a hydraulic crane is highly iterative and a number of iterations are needed to achieve a satisfactory design. The design of a system, containing subsystems from hydraulic and mechanical domains is difficult, and the modeling technique must take into account their interaction in operational performance. The hydraulic actuators, controlling the moving crane elements, have their own dynamics due to the presence of inertial parameters of their elements and the compressibility of the hydraulic oil. The internal forces, which arise in the mechanical system during performance of typical operations, and the pressures and flows in the hydraulic system, are important for the reliability and strength calculations of the crane elements. The main direction for the improvement of the system performance is the implementation of a control system for minimizing the payload swinging, especially for the slewing motion.

The performed validation of the developed dynamical model shows its applicability for the study of the hydraulic crane motion simulation, considering large angles of payload swinging and taking into account the hydraulic driving system dynamics.